Cellular and Molecular Life Sciences (2023) 80:292
https://doi.org/10.1007/s00018-023-04940-3

ORIGINAL ARTICLE

Reciprocal negative feedback regulation of ATF6α and PTEN promotes prostate cancer progression

Tingting Feng[1] · Ru Zhao[1,2] · Hanwen Zhang[1] · Feifei Sun[1] · Jing Hu[2] · Meng Wang[1] · Mei Qi[2] · Ling Liu[2] · Lin Gao[1] · Yabo Xiao[3] · Junhui Zhen[1,2] · Weiwen Chen[4] · Lin Wang[5,6] · Bo Han[1,2]

Received: 23 February 2023 / Revised: 14 July 2023 / Accepted: 4 August 2023 / Published online: 16 September 2023

Abstract

Phosphatase and tensin homolog (PTEN) loss tightly correlates with prostate cancer (PCa) progression and metastasis. Inactivation of PTEN leads to abnormal activation of PI3K/AKT pathway. However, results from clinical trials with AKT inhibitors in PCa have been largely disappointing. Identification of novel regulators of PTEN in PTEN-dysfunctional PCa is urgently needed. Here we demonstrated that the expression level of PTEN is inversely correlated with the signature score of unfolded protein response (UPR) in PCa. Importantly, PTEN suppresses the activity of ATF6α, via interacting to dephosphorylate ATF6α and consequently inhibiting its nuclear translocation. Conversely, ATF6α promotes the ubiquitination and degradation of PTEN by inducing CHIP expression. Thus, ATF6α and PTEN forms a negative feedback loop during PCa progression. Combination of ATF6α inhibitor with AKT inhibitor suppresses tumor cell proliferation and xenograft growth. Importantly, this study highlighted ATF6α as a therapeutic vulnerability in PTEN dysfunctional PCa.

Keywords PTEN · UPR · ATF6α · Prostate cancer

Introduction

Prostate cancer (PCa) is characterized as being histologically and molecularly heterogeneous, with low-risk localized PCa having an indolent natural history, while others have aggressive and lethal disease [1, 2]. Phosphatase and tensin homolog (PTEN) is one of the most commonly inactivated tumor suppressor gene in PCa and its loss is associated with poor clinical outcome [3]. PTEN deficiency, resulting mainly from PTEN deletion or mutation, could be detected in tissues representing all stages of PCa progression, and especially at much higher frequency in metastatic PCa and castration resistant prostate cancer (CRPC) [4–6]. Inactivation of PTEN leads to abnormal activation of PI3K/AKT pathway [7]. Until recently, however, results from clinical trials with AKT inhibitors in PCa have been largely disappointing [8–10]. Therefore, an appropriate design of rational combinations of PI3K/AKT inhibitors with other novel agents is urgently needed. Most recently, Sweeney et al. reported that co-targeting AKT and androgen-receptor

Tingting Feng, and Ru Zhao have Contributed equally to this work.

✉ Lin Wang
linwang@sdfmu.edu.cn

✉ Bo Han
boh@sdu.edu.cn

1 The Key Laboratory of Experimental Teratology, Ministry of Education and Department of Pathology, School of Basic Medical Sciences, Shandong University, Jinan, Shandong, China

2 Department of Pathology, Qilu Hospital, Shandong University, Jinan, Shandong, China

3 School of Basic Medical Sciences, Shandong University, Jinan, Shandong, China

4 Department of Biochemistry and Molecular Biology, School of Basic Medical Science, Shandong University, Jinan, Shandong, China

5 Biomedical Sciences College and Shandong Medicinal Biotechnology Centre, NHC Key Laboratory of Biotechnology Drugs, Key Lab for Rare and Uncommon Diseases of Shandong Province, Shandong First Medical University and Shandong Academy of Medical Sciences, Jinan, Shandong, China

6 Department of Oncology, The First Affiliated Hospital of Shandong First Medical University, Jinan, Shandong, China

signaling pathway was a potential treatment strategy for men with PTEN-loss metastatic CRPC (mCRPC) [11]. Of note, PTEN function is also regulated at the transcriptional, post-transcriptional and translational levels [12–14]. Thus far, it remains largely unknown as to what extent dysregulation of these processes could contribute to PCa progression.

The unfolded protein response (UPR) is a homeostatic mechanism to maintain endoplasmic reticulum (ER) function [15] Over the past decade, a large body of evidence has emerged to support a role of UPR in the establishment and progression of several types of malignancies, including PCa [16, 17]. Recently, an adverse correlation between PTEN and UPR signaling was reported in high-grade serous ovarian carcinoma where knockdown of PTEN leads to increased protein synthesis, upregulation of BiP and elevated levels of p-eIF2α and CHOP [18]. Additionally, in another study, Wang et al. showed that UPR pathway is preferential activated in PTEN-deficient triple negative breast cancer [19]. However, the link between PTEN and UPR is unclear in PCa progression.

The UPR is mediated by at least three well-conserved stress sensors that are ER-localized transmembrane receptors: pancreatic ER kinase-like ER kinase (PERK), inositol-requiring kinase 1 (IRE1), and activating transcription factor 6 (ATF6) [15]. ATF6 consists of two isoform ATF6α and ATF6β, both of which can be activated by ER stress [20]. Upon activation, the N-terminal fragment of ATF6α and ATF6β, designated as ATF6α(N) and ATF6β(N), is spliced from their full-length in the Golgi apparatus and transported into the nucleus to induce gene expression [21]. ATF6α plays a dominant role in inducing the expression of ATF6 target genes. Clinically, Liu et al. suggested that ATF6α is expressed at a higher level in PCa tissues than in benign prostatic hyperplasia (BPH) [22]. In the present study, we found that PTEN expression is adversely related to UPR signature in human PCa tissues. Reintroduction of PTEN into PTEN-deficient LNCaP cells leads to ATF6α dephosphorylation, inhibits its nuclear translocation and transcriptional regulatory activity. In turn, ATF6α could promote PCa progression by destabilizing PTEN protein in CHIP-dependent way. Importantly, co-targeting ATF6α and PI3K/AKT pathways may be a promising therapeutic approach for PCa, especially the ones with PTEN dysfunction.

Methods

Cell culture and reagents

LNCaP, VCaP, DU145, PC3 and HEK293T cell were purchased from American Type Culture Collection (ATCC). All cell lines were authenticated by short tandem repeat analysis and were tested for mycoplasma contamination. The information of reagents is shown in Supplementary Table 1.

Animals

All experimental protocols for animal studies were approved by the Institutional Animal Care and Use Committee of School of Basic Medical Sciences, Shandong University (Document No. ECSBMSSDU2021-2-126) and conducted in accordance with the National Institutes of Health Guide for the Care and Use of Laboratory Animals. Different groups were allocated in a randomized manner and investigators were blinded to the allocation of different groups when doing drug treatment. More detailed information on animals is included in Supplementary Materials and Methods.

Patients and tissue specimens

A total of three tissue microarrays were constructed representing 15 patients with BPH and 130 clinically localized PCa patients who underwent radical prostatectomy between 2012 and 2015 at Qilu Hospital of Shandong University (Jinan, China). Three cores (0.6 mm in diameter) were taken from each representative tumor focus and the morphology was confirmed by two pathologists (J.H. and M.Q). The localized tissues consisted of Gleason score 3 + 3 = 6 (n = 17), Gleason score 3 + 4 = 7 (n = 20), Gleason score 4 + 3 = 7 (n = 24), Gleason score 4 + 4 = 8 (n = 30), and Gleason score ≥ 9 (n = 39) tumors. This study was conducted in accordance with the International Ethical Guidelines for Biomedical Research Involving Human Subjects. This study protocol was approved by Shandong University Medical Research Ethics Committee according to the Declaration of Helsinki (Document No. ECSBMSSDU2021-1–61).

Immunohistochemistry (IHC) and immunofluorescence staining

IHC was carried out as described previous [23]. Detailed information of the IHC protocol as well as evaluation procedure of tissues microarray were provided in Supplementary Materials and Methods. For immunofluorescence, proteins were detected using goat anti-mouse Alexa Fluor 594. For quantitation of ATF6α subcellular distribution, at least 150 cells were scored for each experiment. Cells were rated as showing nuclear staining (N), cytoplasmic staining (C), or staining within both the nucleus and the cytoplasm (N + C). The ATF6α nuclear location (%) = N + (N + C) / total cells. Nuclei were identified by DAPI staining. The information of antibodies was shown in Supplementary Table 2.

Western blot and co-immunoprecipitation

Preparation of cell lysates and performance of western blot and immunoprecipitation were carried out according to our published procedure [24]. Cytoplasmic and nuclear proteins were extracted using the ProteoExtract subcellular proteome extraction kit (#539,791, Millipore). The information of antibodies is summarized in Supplementary Table 2.

RNA isolation and real-time qPCR analysis

Total RNA was extracted using TRIzol reagent according to the manufacturer's protocol (Vazyme Biotech, R401-01 regent kit) and 1 μg of RNA was reverse-transcribed with ReverTra Ace qPCR RT kit (PCR-311, Toyobo). Real-time qPCR was performed using the SYBR Green mix (QPK-201, Toyobo). The primer sequences used are listed in Supplementary Table 3.

Transient transfection and viral transduction

Premade siRNA constructs were purchased from RiboBio (Guangzhou, China) and all the siRNA constructs sequences were list in Supplementary Table 4. For DNA transfections, the plasmid constructs were purchased from Biosun Inc (Jinan, China) and WZ Biosciences Inc (Jinan, China). The transfection procedure was performed as previously described. Human Lenti-ATF6α-GFP and its control Lenti-GFP were obtained from Genecopoeia. To acquire a stable cell line, single-cell clonal isolates were selected by puromycin.

Luciferase reporter gene assay and Chromatin immunoprecipitation (ChIP)

Luciferase activity was determined using the Promega luciferase assay kit (E1910, Promega) following the manufacturer's protocol. Reporter activity was detected using the Molecular devices spectraMzx iD3. ChIP experiments were performed with ChIP assay kit (#17–295, Millipore) according to the manufacturer's protocol. Briefly, Cells were sonicated, pre-cleaned, mixed with magnetic beads and incubated with indicated antibodies. After DNA purification, the enrichment of the DNA template was analyzed by PCR and real-time qPCR using primers. The primers were list in Supplementary Table 5.

Gene set enrichment analysis

We used the java GSEA v4.0 program. GSEA were performed according to the instructions. Gene sets of Hallmark Collection, Canonical Pathway were used. All gene sets are from the Molecular Signatures Database v7.5.1.

Quantification and statistical analysis

All of the statistical details including the statistical tests used, exact number of animals, definition of center, and dispersion and precision measures for the experiments can be found in the figures, figure legends or in the results. All statistical analyses were carried out using GraphPad Prism 8 software (GraphPad software, CA, US). The two-tailed unpaired t-test was used to calculate statistical significance between the two groups. Survival information was verified by Kaplan–Meier analysis and compared using the log-rank test. All results were presented as the mean and the standard error of the mean. *P* values considered to be significant as follows: $*P<0.05$, $**P<0.01$, $***P<0.001$, and $****P<0.0001$.

Results

PTEN expression is adversely related to UPR signature and PTEN deficiency synergizes with ATF6α to activate UPR signaling in PCa cells

To determine the correlation between PTEN expression and UPR signaling pathway in PCa, we have analyzed various PCa public datasets. As shown in Fig. 1a, b, gene set enrichment analysis (GSEA) was performed using microarrays from Gene Expression Omnibus (GEO) datasets (GSE3325 and GSE6919). The UPR gene signature was significantly enriched in *PTEN*-low tumors compared with *PTEN*-high tumors. Of note, ATF6α target genes (*HSPA5* and *PDIA6*) were up-regulated in *PTEN*-low samples (Supplementary Fig. 1a, 1b).

To further confirm the relation between PTEN function and UPR activation, prostate-specific *Pten* knockout (*Pten*$^{flox/flox}$: Pb-Cre^{+}, referred to herein as *Pten*$^{PC-/-}$ mice) mice were used. As shown in Fig. 1c, PTEN protein levels were significantly decreased in wild type (WT) mice under ER stress inducer tunicamycin (Tm) treatment. In addition, spliced ATF6α (ATF6α-N), and its target gene BiP were increased significantly after Tm treatment in *Pten*$^{PC-/-}$ prostate tissues than those in WT mice. To further verify the effects of PTEN on UPR activity, we next silenced PTEN with siRNA in DU145 and VCaP (PTEN-WT) cells and overexpressed PTEN in LNCaP and PC3 (PTEN-deficient) cells. Western blot showed that the protein levels of ATF6α and its target gene were increased after silencing PTEN expression, especially in the presence of Tm treatment in DU145 and VCaP cells (Fig. 1d and Supplementary Fig. 1d). In contrast, PTEN overexpression inhibited protein expression of ATF6α and its target gene induced by Tm in LNCaP and PC3 cells (Fig. 1e and Supplementary Fig. 1e). Of note, compared to the changes of phosphorylated levels

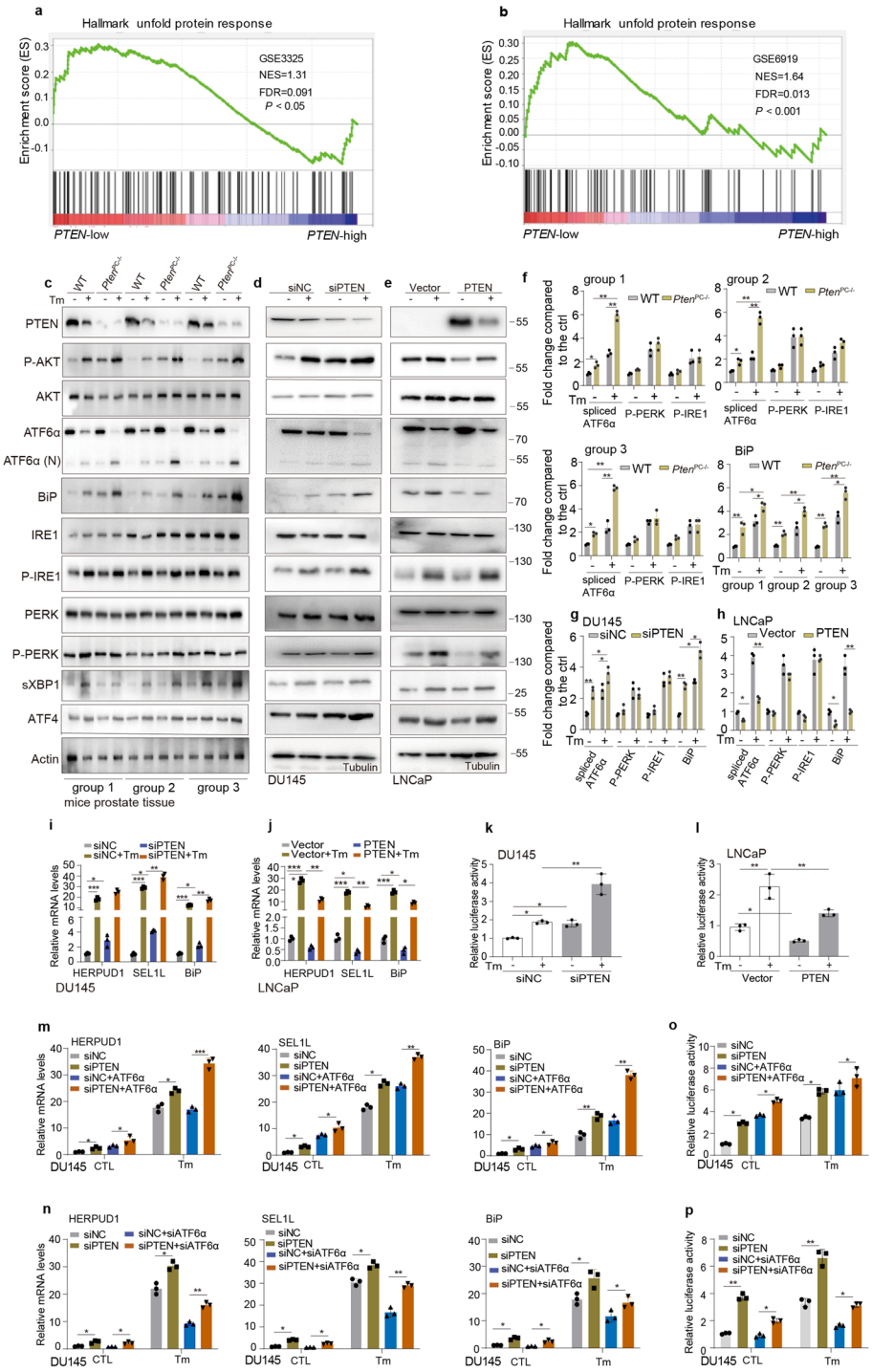

of IRE1 (p-IRE1) and PERK (p-PERK), the ATF6α protein levels in spliced form increased more significantly in *Pten*$^{PC-/-}$prostate tissues (Fig. 1f–h). Real-time qPCR revealed that mRNA levels of the ATF6α target genes were suppressed by overexpression PTEN in LNCaP cells and activated by silence PTEN in DU145 cells (Fig. 1i, j and Supplementary Fig. 1 g). Additionally, as shown in Fig. 1k, l, the BiP luciferase activity was highly induced by Tm. However, these activity effects of Tm were further enhanced by PTEN silencing in DU145 cells but decreased by PTEN overexpression in LNCaP cells. Collectively, these results demonstrated that ATF6α signaling was adversely related to PTEN expression.

Further analyses on The Cancer Genome Atlas (TCGA) and GSE29010 showed that UPR gene signature was enriched in PTEN-loss prostate tumors when compared

◂**Fig. 1** PTEN expression is adversely related with UPR gene signature and PTEN deficiency synergizes with ATF6α to activate UPR signaling in PCa cells. **a**, **b** GSEA of the UPR gene signature in GSE3325 and GSE6919 datasets, where genes were ranked by fold changes between *PTEN* low versus *PTEN* high in descending order. According to the *PTEN* expression levels, we arbitrarily defined the top 50% as the *PTEN* high group and the bottom 50% as the *PTEN* low group. GSEA, gene set enrichment analysis; NES, normalized enrichment score; FDR, false discovery rate. **c** Western blot analysis of the UPR related gene in the prostate tissues from WT (n = 6) or *Pten* $^{PC-/-}$ (n = 6) mice. P-AKT as a positive control to evaluate the efficiency of PTEN overexpression or silencing. WT, wild type; NC, negative control; group mice: every group mouse consists of four mice in total: WT mouse without Tm treatment, WT mouse with Tm treatment, *Pten* $^{PC-/-}$ mouse without Tm treatment and *Pten* $^{PC-/-}$ mouse with Tm treatment. **d**, **e** DU145 and LNCaP cells were transfected with indicated plasmid or siRNA followed by adding Tm (2.5 μM) for additional 12 h as indicated. Whole cell lysates were subjected to immunoblot with indicated antibodies. **f**–**h** Band intensity of ATF6α(N), P-PERK, P-IRE1α and BiP were measured using Image J software, presented as fold change compared with untreated WT, siNC or Vector respectively. **i**, **j** Cells as in (d-e) were harvested and real-time qPCR analyses were performed with primers of ATF6α target genes. **k**, **l** Cells as in (d-e) were harvested and the BiP promoter activity was identified by luciferase reporter assay. **m**, **n** DU145 cells were transfected with siRNA against PTEN. At 24 h post transfection, cells were transfected with ATF6α expression plasmid (m) or siRNA against ATF6α (n) and incubated for additional 48 h followed by adding Tm for another 6 h. Real-time qPCR analyses were then performed with primers of ATF6α target genes. CTL: Control. **o**, **p** Cells as in (m–n) were harvested and the BiP promoter activity was identified by luciferase reporter assay. Each data point represents one independent observation. Data represent mean ± SEM. P values were determined by two-tailed unpaired Student's t test; * $P < 0.05$, ** $P < 0.01$, *** $P < 0.001$

with PTEN-WT prostate tumors (Supplementary Fig. 1 h, 1i). We next analyzed the relationship between PTEN loss and ATF6α, PERK and IRE1 pathway signature. As shown in Supplementary Fig. 1j, ATF6α signature was significantly enriched in Pten-low tumors ($P = 0.027$), whereas the enrichment of IRE1 ($P = 0.062$) and PERK ($P = 0.31$) pathways is not statistically significant [25]. Additionally, compared with that of PERK or IRE1 knockdown, the proliferation induced by PTEN knockdown could be attenuated more significantly after ATF6α knockdown (Supplementary Fig. 1 k). Collectively, these results supported that PTEN dysfunction can activate the ATF6α signaling.

Since ATF6α could be activated by PTEN knockout or knockdown, we aimed to confirm whether PTEN dysfunction participated in the activity of ATF6α signaling. As shown in Fig. 1m, the combination of PTEN silencing and ATF6α overexpression significantly increased mRNA levels of *HERPUD1*, *SEL1L*, and *BiP* in DU145 cells. However, the increase induced by PTEN silencing could be attenuated when ATF6α was silenced (Fig. 1n). Likewise, we identified that the increase of the luciferase activity of BiP promoter caused by PTEN knockdown could be further strengthened by introducing ATF6α (Fig. 1o) but abolished by silencing ATF6α in DU145 cells (Fig. 1p).

ATF6α protects against ER stress-induced cytotoxicity and promotes PCa progression in vivo

To investigate the correlation between PTEN and ATF6α in clinical PCa samples, we performed IHC assay analysis using 145 Chinese PCa cases from Qilu hospital with three tissue microarrays (TMAs). We found that the ATF6α protein expression was mainly localized in the cytoplasm in BPH samples. Of note, nuclear staining of ATF6α was frequently seen in PCa cases with high Gleason score accompanied with PTEN loss. Representative image of IHC staining for nuclear ATF6α expression of PCa cases were shown in Fig. 2a. A positive correlation between nuclear ATF6α expression with Gleason score was shown in Fig. 2b. Furthermore, high expression of ATF6α was significantly associated with poor clinical outcome (Fig. 2c). We also observed that the expression levels of ATF6α target genes were significantly higher in localized PCa than those in BPH tissues as shown in GSE46602 and GSE70768 (Supplementary Fig. 2a). And the Kaplan–Meier curve showed that patients with high levels of ATF6α target genes had a shorter biochemical relapse free survival rate than those with low expression (Supplementary Fig. 2b). In all, these results suggested that upregulation of ATF6α target gene was associated with PCa progression to advanced clinical states. To elucidate the biological functions of ATF6α in PCa cells, we designed siRNA against ATF6α (siATF6α). As shown in Supplementary Fig. 2c, 2d, siATF6α can significantly deplete mRNA and protein expression levels of ATF6α in DU145 and LNCaP cells, accordingly. Notably, apoptosis could be induced when PCa cells were transiently transfected with ATF6α expression plasmid (5 μg). However, the growth rates of PCa cells that were transiently transfected with ATF6α expression plasmid (2.5 μg) or the ones with stable ATF6α overexpression was higher than those of their parental controls (Supplementary Fig. 2e, 2f). It could be inferred that the role of ATF6α in cellular destiny showed a dose- or context dependent manner. Thus, the dose of ATF6α expression plasmid (2.5 μg) was selected for subsequent experiments. We showed that Tm treatment could significantly reduce cell colony formation and cell proliferation whereas increase apoptosis of DU145 cells compared with control (Fig. 2d and Supplementary Fig. 2j-2 k). Additionally, the inhibitory effects of Tm on cell colony formation were further enhanced by treatment with ATF6α siRNA or its inhibitor but compromised by ATF6α overexpression (Fig. 2d). Next, in vivo experiments demonstrated that, introduction of ATF6α into DU145 cells showed an increased tumor growth

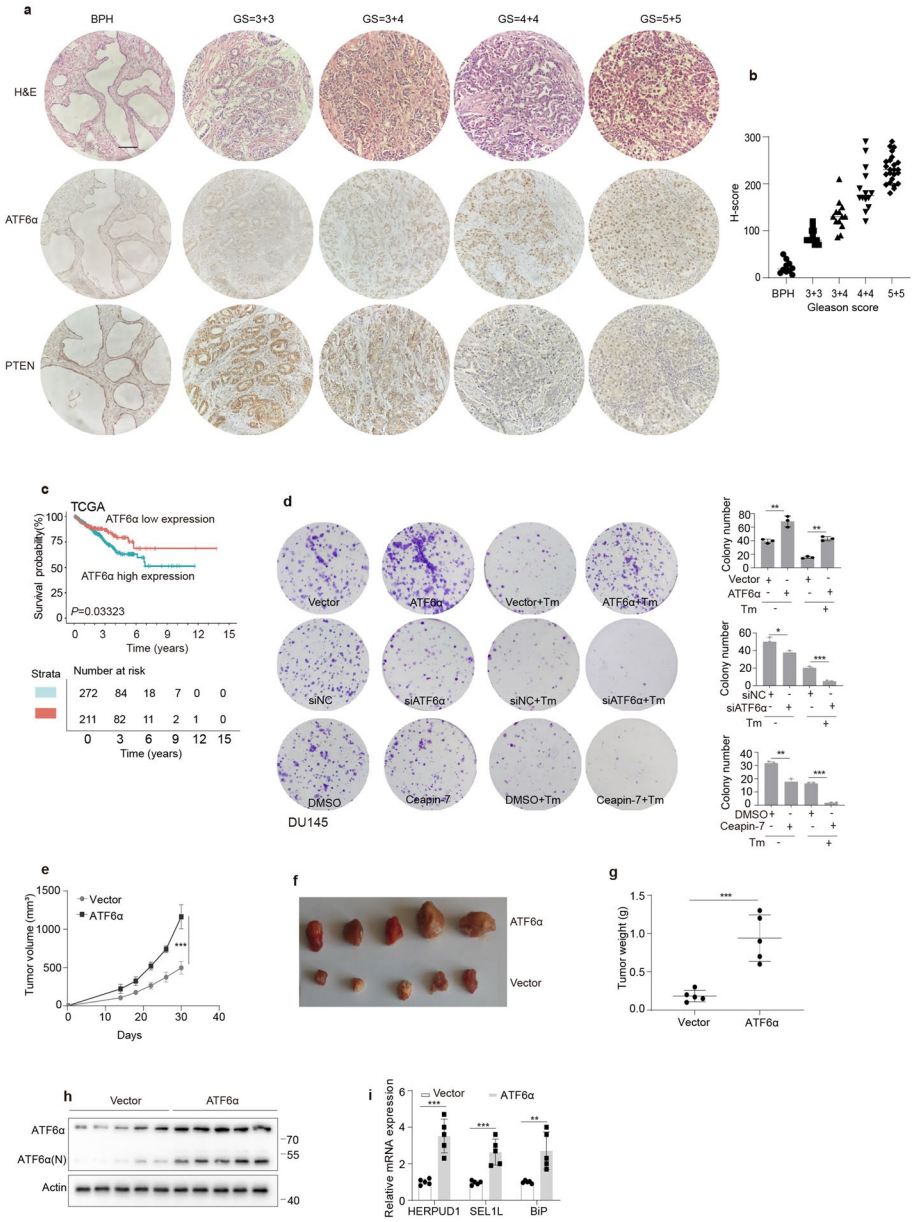

Fig. 2 ATF6α protects against ER stress-induced cytotoxicity and promotes PCa progression in vivo. **a**, **b** Protein expression of PTEN and ATF6α in BPH and PCa tumor specimens. **a** Upper: Representative H&E images of BPH and PCa cases with different GS (original magnification, 400×). Middle & Bottom: Representative IHC staining of PTEN and ATF6α in BPH and PCa cases with different GS (original magnification, 400×). **b** H-scores for ATF6α nuclear expression in BPH and PCa cases with different GS. Scale bars, 50 μm. BPH, Benign prostatic hyperplasia; GS, Gleason score. **c** Kaplan–Meier analysis comparing overall survival of PCa patients with low and high ATF6α expression in TCGA cohort. **d** DU145 cells were transfected with ATF6α overexpression plasmid or siRNA against ATF6α for 24 h or pretreated with ATF6α inhibitor Ceapin-A7 for 12 h and then were treated with 2.5 μM Tm. Cell colony formation ability was then measured. **e–g** DU145 cells stably expressing ATF6α or vector were subcutaneously injected into the backs of nude mice (n = 5). Tumor size was measured three times a week. At the endpoint, tumors isolated from euthanized mice were weighed and photographed. **h**, **i** The levels of endogenous ATF6α and its target genes in the excised tumors were determined by western blot and real-time qPCR analysis. Each data point represents one independent observation. Data represent mean ± SEM. P values were determined by two-tailed unpaired Student's t test; * $P < 0.05$, ** $P < 0.01$, *** $P < 0.001$

in the xenograft models when compared to its parental controls ($998 \pm 145.6 mm^3$ *vs.* $456 \pm 93\ mm^3$) (Fig. 2f, h). Moreover, the protein levels of ATF6α and its target genes in DU145-ATF6α group were relatively increased compared with that in DU145-vector group (Fig. 2i, j). Collectively, our data suggested that ATF6α contributes to PCa progression.

PTEN interacts with ATF6α and inhibits ATF6α activity

To elaborate on the effect of PTEN on ATF6α, we sought to determine whether ATF6α physically associates with PTEN. As shown in Fig. 3a, HA-PTEN co-precipitated with the full-length Flag-ATF6α (short for ATF6α(P)), but not the N-terminal of ATF6α (short for ATF6α(N)) in LNCaP cells. Interestingly, Tm diminished the interaction between HA-PTEN and ATF6α(P). Additionally, the endogenous interaction between ATF6α(P) and PTEN in DU145 cells dramatically decreased with the presence of Tm (Fig. 3b). Finally, to determine whether PTEN directly interacts with ATF6α, GST, and recombinant GST-ATF6α were used to pull down the lysates of HEK293T cells with HA-PTEN overexpression. As shown in Fig. 3c, GST-ATF6α, but not GST protein, interacted with PTEN.

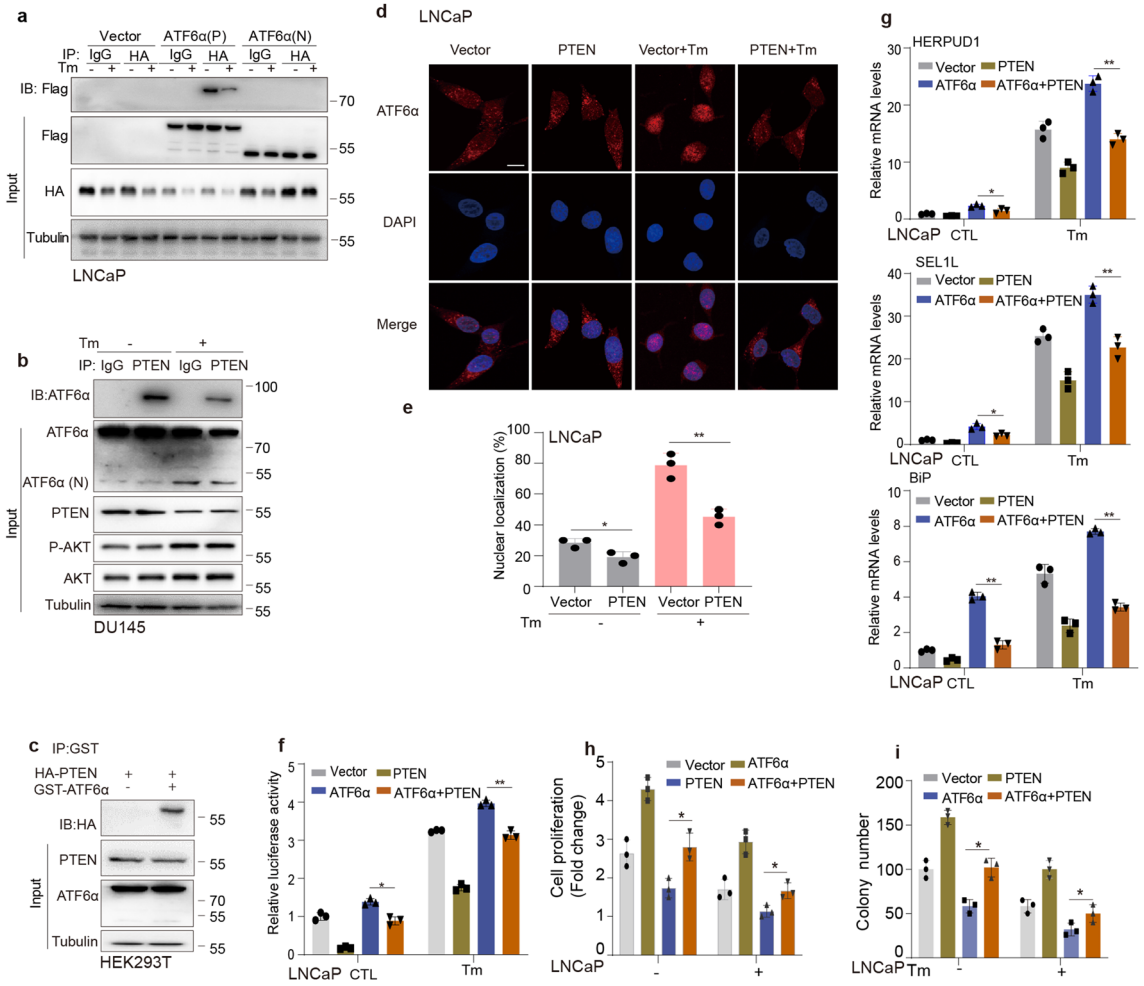

Fig. 3 PTEN interacts with ATF6α and inhibits ATF6α activity. **a** LNCaP cells were transfected with flag-ATF6α full length, flag-ATF6α N terminal or empty vector. After 24 h, cells were transfected with HA-PTEN for another 48 h followed by adding Tm (2.5 μM) for another 6 h. Cells were then lysed and subjected to immunoprecipitation using anti-HA antibody. ATF6α(P): ATF6α full length plasmid; ATF6α(N): ATF6α N terminal plasmid. **b** Co-precipitation between endogenous ATF6α and PTEN in DU145 cells treated with Tm for 6 h. **c** HEK293T cells were transfected with HA-PTEN and cell lysates were incubated with GST or GST-ATF6α fusion protein and the direct association of ATF6α with PTEN was detected. **d** LNCaP cells were transfected with PTEN or empty vector. At 48 h post transfection, the cells were treated with Tm for 6 h and then staining with ATF6α antibody (red). Nuclei were counterstained with DAPI (blue). Scale bar, 100 μm. **e** Quantitative analysis of ATF6α nuclear localization as shown in 3d. **f** LNCaP cells were transfected with PTEN expression plasmid. After 24 h, cells were transfected with ATF6α expression plasmid and then followed by adding Tm for another 6 h. BiP promoter activity was evaluated by luciferase reporter assay. **g** LNCaP cells were transfected with ATF6α expression plasmid. At 24 h post transfection, cells were transfected with PTEN expression plasmid and incubated for additional 48 h followed by adding Tm for another 6 h. ATF6α target genes were analyzed by real-time qPCR. **h**, **i** Following indicated treatment as in (g), the proliferation rates and colony formation number were measured by MTT and colony formation assays. Each data point represents one independent observation. Data represent mean ± SEM. P values were determined by two-tailed unpaired Student's t test; * $P < 0.05$, ** $P < 0.01$

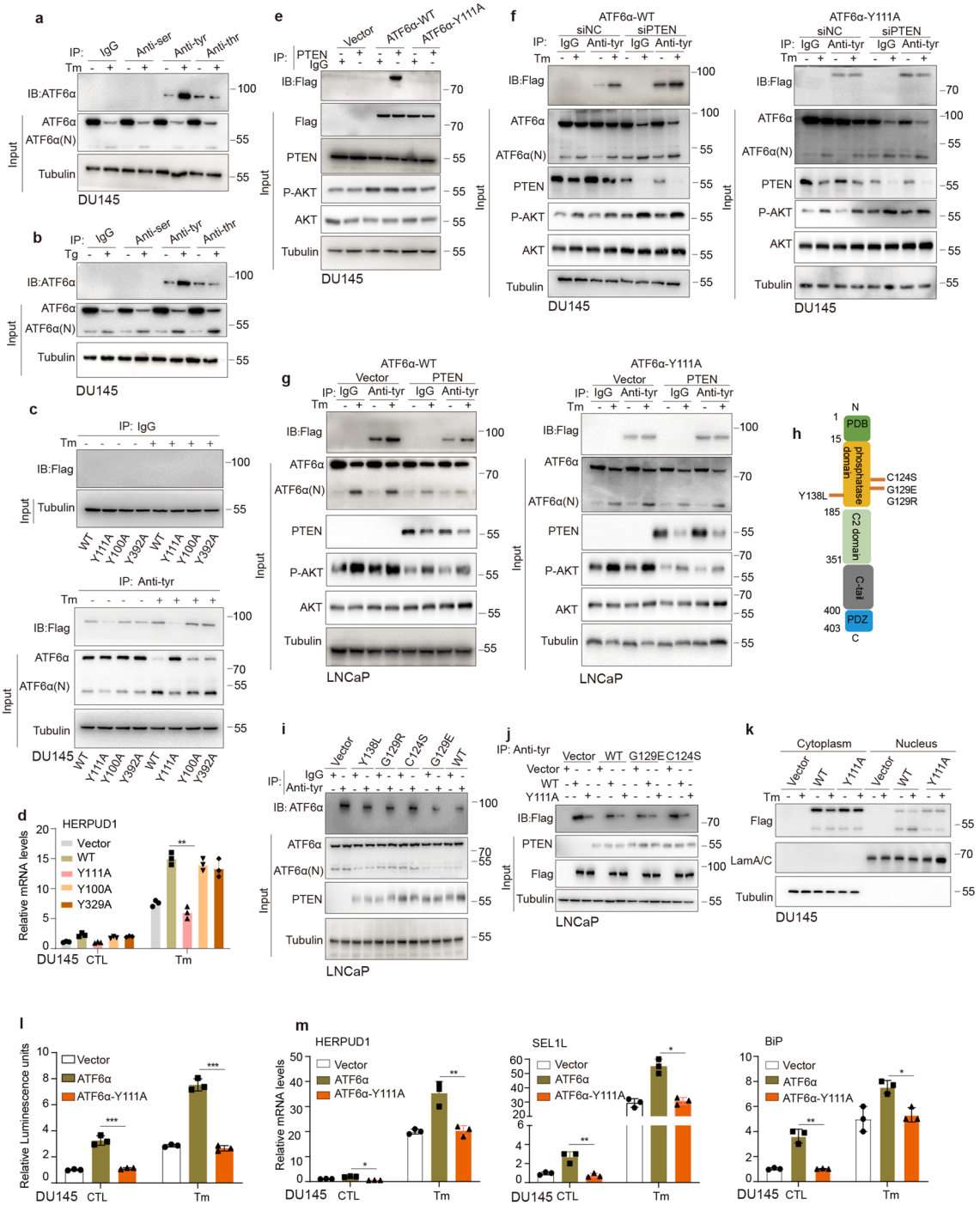

Together, these results demonstrated the direct interaction between ATF6α and PTEN.

Immunofluorescent staining analysis showed that the nuclear staining of ATF6α markedly increased when LNCaP cells were treated with Tm, whereas the staining of ATF6α in nucleus significantly decreased when PTEN was overexpressed (Fig. 3d, e). We then investigated whether PTEN could inhibit the transcriptional activity of ATF6α using a BiP promoter-luciferase system. As shown in Fig. 3f, introducing PTEN profoundly diminished the transcriptional activity of BiP promoter in LNCaP cells with overexpression ATF6α. Likewise, PTEN can significantly suppress the mRNA levels of *HERPUD1*, *SEL1L*, and *BiP* induced by ATF6α overexpression in LNCaP cells (Fig. 3g).

We then performed rescue experiments to determine whether ATF6α could reverse the proliferation-inhibiting effect induced by PTEN overexpression. As shown in Fig. 3h and Supplementary Fig. 3a, 3b, ectopic PTEN could

◂**Fig. 4** ATF6α activity was repressed by PTEN mediated-phosphatase activity. **a**, **b** DU145 cells were treated with or without Tm (2.5 μM) (**a**) or Thapisigargin (Tg) (0.5 μM) (**b**) for 6 h. Whole lysates were then subjected to immunoprecipitation using anti-phospho-serine (ser), tyrosine (tyr), and threonine (thr) specific antibodies. **c** DU145 cells were transfected with flag-ATF6α^{WT} or flag-ATF6α mutants (Y111A, Y100A, Y392A) with or without Tm for 6 h. Whole lysates were then subjected to immunoprecipitation using anti-phosphotyrosine antibody. **d** Cell as in (**c**) and then the expression of ATF6α target gene were measured by real time-qPCR. **e** The binding between PTEN and flag-ATF6α^{WT} or flag-ATF6α^{Y111A} were performed using co-immunoprecipitation assays in DU145 cells transfected with flag-ATF6α^{WT} or flag-ATF6α^{Y111A}. **f**, **g** DU145 cells were transfected with siRNA against PTEN (f) and LNCaP cells were transfected with PTEN expression plasmid (**g**) for 24 h and then introduced with flag-ATF6α^{WT} or flag-ATF6α^{Y111A} plasmids for 48 h, followed by treatment of Tm for 6 h. Tyrosine phosphorylation levels of ATF6α were then measured by immunoprecipitation and western blot. **h** A graphical representation of the PTEN domain structure. Mutations in the phosphatase and tail domains, including C124S (phosphatase-dead), G129R (phosphatase-deficient), Y138L (protein phosphatase dead), G129E (lipid-phosphatase dead) were shown. **i** LNCaP cells were transfected with empty vector, PTEN^{WT}, or PTEN mutants (Y138L, G129R, C124S, or G129E) for 48 h. Cells were then lysed and subjected to immunoprecipitation using anti-phosphotyrosine antibody. **j** DU145 cells were transfected with PTEN^{WT}, PTEN mutation overexpression plasmid (C124S or C129E) for 24 h and then introduced with flag-ATF6α^{WT} or flag-ATF6α^{Y111A} for 48 h. Tyrosine phosphorylation levels of ATF6α were then measured by immunoprecipitation. **k** Cytoplasmic and nuclear ATF6α protein levels in DU145 cells transfected with flag-ATF6α^{WT} or flag-ATF6α^{Y111A} in the presence or the absence of Tm for 12 h were analyzed by western blot. **l**, **m** Cells as in (**k**) and then BiP promoter activity was measured by luciferase reporter assay (**l**) and the mRNA levels of *HERPUD1*, *SEL1L*, and *BiP* (**m**) were analyzed by real-time qPCR. Each data point represents one independent observation. Data represent mean ± SEM. P values were determined by two-tailed unpaired Student's t test; * $P<0.05$, ** $P<0.01$, *** $P<0.001$

decrease the cellular proliferation of LNCaP, PC3, VCaP and DU145. However, such decrease could be partially restored by ectopic overexpression of ATF6α, suggesting that ATF6α could promote cell growth, at least in part, by deregulating PTEN. Accordingly, colony formation assay also confirmed that ATF6α reverses the inhibition of PTEN-induced cell colony formation (Fig. 3i and Supplementary Fig. 3c). Furthermore, overexpression of ATF6α could increase the cell proliferation of PCa cells with PTEN deficiency, which indicates that ATF6α may enhance cell growth independently of PTEN. Since BiP has been shown to control ATF6α export from ER through a dissociation mechanism, we next determined whether PTEN plays a role in their dissociation. The interaction between ATF6α and BiP was determined by immunoprecipitation. In consistent with the previous study, ATF6α dissociated from BiP when PCa cells were challenged with Tm. However, there was no visible change in dissociation when PTEN was overexpressed in LNCaP cells (Supplementary Fig. 3d) or knocked down in DU145 cells (Supplementary Fig. 3e). The micro-scale thermophoresis assay also showed that PTEN failed to affect the binding between BiP and ATF6α (Supplementary Fig. 3f). This suggested that the dissociation between BiP and ATF6α is not affected by PTEN.

ATF6α activity was repressed by PTEN mediated-phosphatase activity

We subsequently explored the molecular basis by which PTEN inactivates ATF6α. Since PTEN is a protein phosphatase that inactivates protein function by dephosphorylation [26, 27], we first determined whether ATF6α could be phosphorylated or not in PCa cells. Our results shown that the tyrosine phosphorylation levels of ATF6α were dramatically increased when DU145 cells were stimulated by Tm and Tg (Fig. 4a, b and Supplementary Fig. 4a). To define the exact phosphorylation site on ATF6α, we constructed several plasmids targeting the tyrosine sites of ATF6α. The results showed that compared with ATF6α^{WT}, the expression levels of phosphorylated and spliced ATF6α were decreased more significantly in ATF6α^{Y111A} in the presence of Tm (Fig. 4c and Supplementary Fig. 4b). Concordantly, real-time qPCR analysis demonstrated that the expression level of *HERPUD1* was significantly decreased in ATF6α^{Y111A} group than ATF6α^{WT} (Fig. 4d). In addition, PTEN only pulled down ATF6α^{WT} but not ATF6α^{Y111A}, which suggests that Y111 is required for its interaction with PTEN (Fig. 4e). To examine whether PTEN dephosphorylates ATF6α or not, PTEN was silenced in DU145 (Fig. 4f) or overexpressed in LNCaP cells (Fig. 4g). The levels of phosphorylated ATF6α(P) were significantly increased in DU145 cells but decreased in LNCaP cells compared with their control. However, no observable change was detected when PTEN as silenced or overexpressed in DU145 or LNCaP cells with mutant ATF6α^{Y111A} (Fig. 4f, g). In addition, the in vitro phosphatase assay also showed that the phosphorylated levels could not be disturbed in ATF6α^{Y111A} compared to its wild type control (Supplementary Fig. 4c), indicating tyrosine residue Y111 is important for the phosphorylation of ATF6α.

To further confirm the specific phosphatase sites of PTEN for ATF6α inactivating dephosphorylation, we transfected LNCaP cells with a variety of PTEN expression constructs with mutations diagramed in Fig. 4h. These mutations include the protein phosphatase dead PTEN^{Y138L}, the lipid phosphatase-dead PTEN^{G129E}, dual phosphatase-deficient PTEN^{C124S}, and PTEN^{G129R} constructs. After transfection with PTEN^{G129E}, the levels of phosphorylated ATF6α were reduced in LNCaP cells (Fig. 4i). Next, we also observed that PTEN^{WT} and PTEN^{G129E} could dephosphorylate ATF6α directly in vitro (Supplementary Fig. 4d). In addition, none of the PTEN constructs affected ATF6α^{Y111A} phosphorylation levels (Fig. 4j). Collectively, these data indicated that PTEN inhibits ATF6α activation by dephosphorylation. To

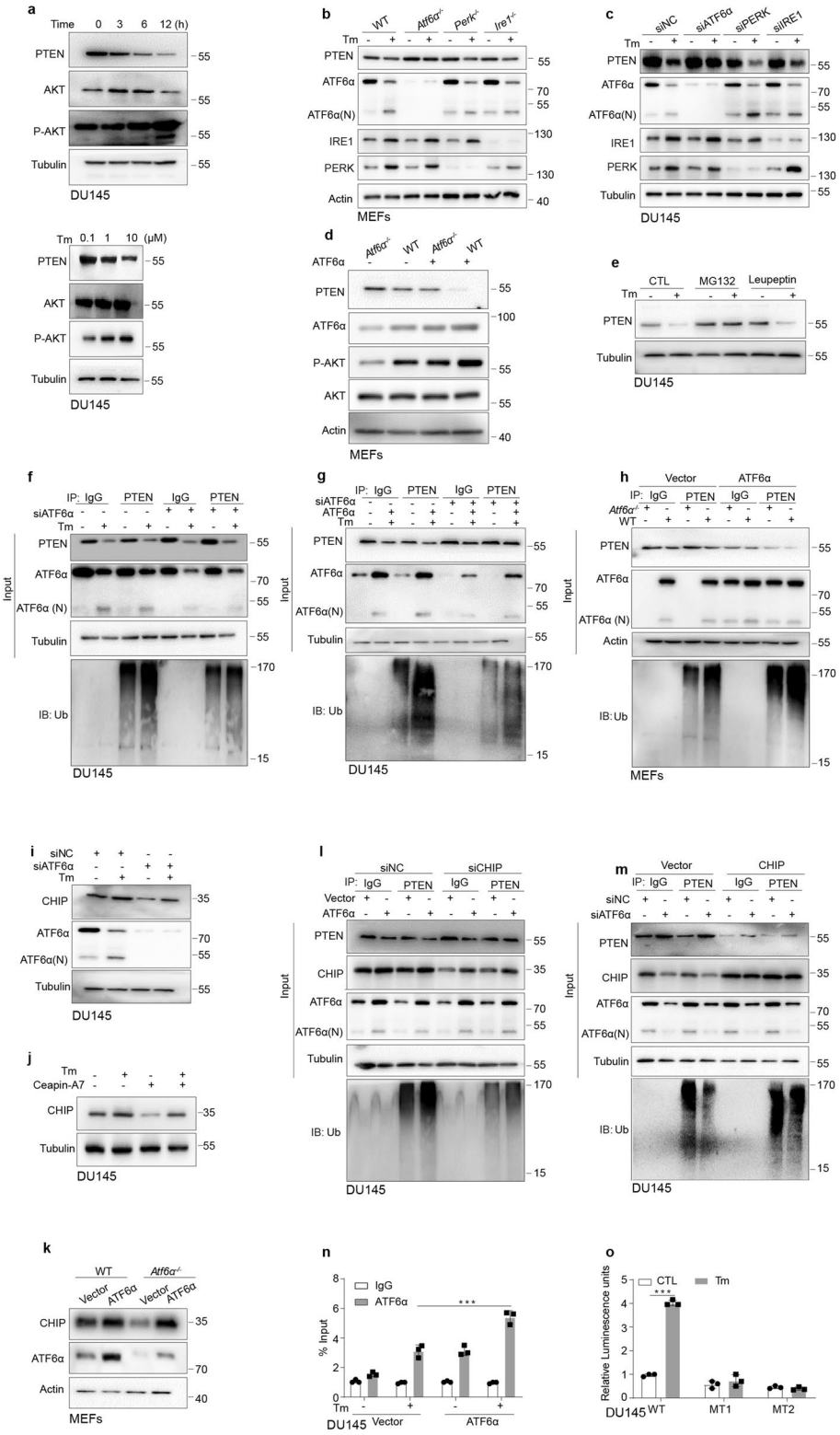

examine the functional consequence of PTEN-mediated dephosphorylation of ATF6α, we analyzed its nuclear translocation in DU145 cells. Our data showed that ATF6α^{WT}, but not ATF6α^{Y111A} was transported into the nucleus in the presence of Tm (Fig. 4k). Furthermore, as shown in Fig. 4l, ATF6α^{Y111A} exhibited low transcriptional activity in both unstressed and stressed cells when compared with ATF6α^{WT}, which was consistent with the results obtained

◂**Fig. 5** ER stress induces PTEN protein instability through ATF6α and ATF6α destabilizes PTEN protein via CHIP-mediated polyubiquitin. **a** DU145 cells was treated with Tm (2.5 μM) in indicated time or concentration, indicated antibodies were tested by western blot. **b**, **c** PTEN protein levels were detected by western blot in WT, *Atf6α*$^{-/-}$, *Perk*$^{-/-}$, and *Ire1*$^{-/-}$ MEFs (**b**) and in DU145 cells with ATF6α, PERK or IRE1 knockdown. **d** *Atf6α*$^{-/-}$ MEFs were transfected with ATF6α expression plasmid and then treated with Tm (2.5 μM) for additional 6 h, indicated antibodies were tested by western blot. **e** DU145 cells were treated with Tm (2.5 μM) for 6 h and then treated with vehicle, 20 μM MG132 or 20 μM Leupeptin for additional 6 h. PTEN protein levels were detected by western blot. **f** DU145 cells were transfected with siRNA against ATF6α for 48 h and then were treated with Tm for another 6 h. Cell lysates were subjected to immunoprecipitation using anti-PTEN antibody. **g** DU145 cells were transfected with siRNA against ATF6α for 24 h and then transfected with ATF6α expression plasmid for another 48 h followed by adding Tm for another 6 h. Cells were then lysed and subjected to immunoblotting using anti-PTEN antibody. **h** Cell as in (**d**) and then cell lysates were performed immunoprecipitation with PTEN antibody. **i** Cell as in (**f**) and then cells were lysed and blotted for CHIP and tubulin. **j** DU145 cells were pretreated with Ceapin-A7 for 12 h and then treated with Tm for another 6 h. Cell lysates were subjected to immunoprecipitation using anti-CHIP antibody. **k** WT and *Atf6α*$^{-/-}$ MEFs were transfected with ATF6α expression plasmid for 48 h, cells were lysed and blotted for CHIP and actin. **l** DU145 cells were transfected with ATF6α expression plasmid for 24 h and then transfected with siRNA against CHIP for another 48 h. Cells were then lysed and subjected to immunoprecipitation using anti-PTEN antibody. **m** DU145 cells were transfected with siRNA against ATF6α for 24 h and then transfected with CHIP expression plasmid for another 48 h. Cells were then lysed and subjected to immunoprecipitation using anti-PTEN antibody. **n** ChIP analysis of CHIP was performed in DU145 cells transfected with overexpression ATF6α plasmid for 48 h followed by adding Tm for another 6 h. **o** DU145 cells were transfected with a reporter plasmid containing the luciferase gene fused with intact or mutant CHIP promoters for 48 h, CHIP promoter activity was then quantified by dual-luciferase reporter assays. Each data point represents one independent observation. Data represent mean ± SEM. P values were determined by two-tailed unpaired Student's t test; *** $P < 0.001$

from real-time qPCR of *HERPUD1*, *SEL1L*, and *BiP* (Fig. 4m). These results highlighted that PTEN-inactivity-mediated phosphorylation is required for the protein cleavage, nuclear translocation, and the subsequent transcription modulation of ATF6α.

ER stress induces PTEN protein instability through ATF6α and ATF6α destabilizes PTEN protein via CHIP-mediated polyubiquitin

Since a significant decrease in PTEN protein levels were observed in mice prostate tissues in the presence of Tm (Fig. 1c), we then treated DU145 and VCaP cells with ER stress inducers in vitro. We found that there was a progressive reduction in PTEN expression in a time- and dose-dependent manner at the protein levels (Fig. 5a and Supplementary Fig. 5b) but not at the mRNA levels (Supplementary Fig. 5c), suggesting the potential of posttranslational modification. We then aimed to determine of which the UPR signaling pathways (ATF6α, PERK, and IRE1) was required for the decrease of PTEN expression by using MEFs from *Atf6α*, *Perk,* and *Ire1* knockout mice. Our data showed that the reduction of PTEN protein levels caused by Tm challenge could be partly reversed in *Atf6α*$^{-/-}$ MEFs compared with those in *Perk*$^{-/-}$ and *Ire1*$^{-/-}$ MEFs (Fig. 5b). Similar effects were also observed when ATF6α, PERK or IRE1 was silenced in DU145 cells (Fig. 5c). However, PTEN protein levels could be rescued after introducing Atf6α into *Atf6α*$^{-/-}$ MEFs (Fig. 5d). Collectively, these results suggest that Tm-induced decrease of PTEN protein expression was mediated by ATF6α.

To characterize the inhibitory effect of Tm on PTEN expression, we treated DU145 cells with MG132 (a proteasome inhibitor) or leupeptin (a protease inhibitor). Our data showed that MG132, but not leupeptin, could rescue Tm-induced PTEN protein levels downregulation (Fig. 5e and Supplementary Fig. 5d). This suggested that PTEN protein undergoes degradation in a proteasome-dependent manner in the presence of Tm. Our results were consistent with previous report, which demonstrated that PTEN protein levels were regulated by both polyubiquitylation and monoubiquitylation[28]. Further analysis showed that more polyubiquitination in PTEN protein occurred in the presence of Tm stimulation or ATF6α overexpression in DU145 cells (Fig. 5f, g). Moreover, polyubiquitination of PTEN proteins could hardly be detected in *Atf6α*$^{-/-}$ MEFs when compared to WT (Fig. 5h). However, such decrease in polyubiquitination could be restored by introducing ATF6α into *Atf6α*$^{-/-}$ MEFs (Fig. 5h). These results confirmed that ATF6α plays an important role in PTEN degradation induced by Tm.

We further investigated the molecular mechanism by which ATF6α mediated PTEN suppression. It was previously reported that CHIP, NEDD4-1, XIAP, and WWP-2 [29–32] regulated PTEN by promoting protein degradation. To search for genes that participate in PTEN degradation induced by ATF6α, we performed real-time qPCR assay in DU145 cells treated with Tm. The data showed that the increase of CHIP mRNA levels in DU145 cells induced by Tm could be reduced by silencing ATF6α (Supplementary Fig. 5e). This result was also confirmed by western blot (Fig. 5i, j and Supplementary Fig. 5f). Furthermore, CHIP protein levels were decreased more significantly in *Atf6α*$^{-/-}$ MEFs, compared with those of *Perk*$^{-/-}$ and *Ire1*$^{-/-}$ MEFs (Supplementary Fig. 5 g). However, such inability in *Atf6α* $^{-/-}$ MEFs could be rescued by introducing ATF6α (Fig. 5k). These data supported that ATF6α was important for protecting CHIP protein stability. We next aimed to assess whether ATF6α destabilizes PTEN protein via CHIP-mediated polyubiquitination. As shown in Fig. 5l, the knockdown of CHIP expression inhibited PTEN

polyubiquitination induced by ATF6α in DU145 cells. Similarly, the decreased PTEN polyubiquitination caused by ATF6α knockdown could be reversed by introducing CHIP expression in DU145 cells (Fig. 5m).

To determine whether ATF6α directly regulates CHIP expression, we conducted a luciferase activity assay with CHIP promoter containing reporter plasmid. Our data showed that Tm treatment could significantly increase the transcriptional activity of CHIP promoter, which also could be enhanced by overexpressing ATF6α (Fig. 5n). It was previously reported that TGAC is the core sequence critical for ATF6α binding [33]. We aligned this sequence with CHIP promoter from − 2000 ~ + 300 bp and found two perfectly matched sequences. We constructed two TGAC-mutant plasmids and performed transient transfection assays with Tm treatment. As shown in Fig. 5o, mutant construct failed to affect CHIP activity in the presence of Tm.

To determine which one plays more important role in PTEN-ATF6α loop in vitro, we transfected DU145 cells with PTEN or ATF6α overexpression plasmid for 48 h followed by ATF6α or PTEN overexpression. Cell colony formation ability was then evaluated. As shown in Supplementary Fig. 5 h, PTEN reduced cell colony number by 50–60% in ATF6α overexpression cells, while ATF6α rescued colony number by 30% in PTEN overexpression cells irrespectively of ER stress inducers. These results implied that PTEN overweighs ATF6α in deregulating PCa progression.

Combined inhibition of ATF6α and AKT synergistically delays PCa progression

In the context of PTEN inactivity, the most pronounced signaling event is the constitutive activation of AKT which associates with the UPR pathway [34]. Indeed, we identified that silencing ATF6α could attenuate the activation of PI3K/AKT pathway in DU145 cells (Fig. 6a). Similar effects were also observed in *Atf6α*$^{-/-}$ MEFs when compared with WT MEFs (Fig. 6b). Furthermore, the decreased activity of AKT signaling elicited by ATF6α deficiency was rescued by re-introducing ATF6α in *Atf6α*$^{-/-}$ knockout MEFs (Fig. 6c). Either PTEN silencing or ATF6α overexpression enhanced AKT activity in DU145 cells, and the combination of them was more effective in increasing AKT activity (Fig. 6d).

We then evaluated the potential benefit of co-targeting ATF6α and AKT in PCa cells. As shown in Fig. 6e, combination of AKT inhibitor (AZD5363) with ATF6α inhibitor (Ceapin-A7) was more effective in inhibiting cell proliferation in DU145 and VCaP cells. Similar to the pharmacologic inhibition, siATF6α combined with AKT inhibitor treatment significantly reduced cell proliferation of PCa cells (Fig. 6f).

To determine the impacts of AZD5363 and Ceapin-A7 on tumor growth, we have established DU145 xenograft model. As shown in Fig. 6g–i, either AZD5363 or Ceapin-A7 treatment reduced the tumor volume, and a combination of AZD5363 and Ceapin-A7 induced further inhibition in tumor growth. The expression level of activated ATF6α was detected by western blot and real-time qPCR assay in these tumors (Fig. 6j, k). These results suggested that ATF6α inhibitor combined with AKT inhibitor would be useful for the treatment of PCa.

Discussion

PTEN is one of the most frequently mutated, deleted, and functionally inactivated tumor suppressor gene in PCa. Loss of PTEN is an important event in prostate carcinogenesis and represents one hallmark of PCa [35]. Clinically, deletion or mutation of at least one PTEN allele was reported to occur in 20–40% of localized cancers and up to 60% of metastases [5]. PTEN inactivation is strongly linked to advanced PCa progression and poor clinical outcome.

Given the high frequency of PTEN loss in PCa, therapeutic strategies that exploit the functional loss of PTEN may prove to be efficacious against PTEN-deficient PCa. Inactivation of PTEN leads to abnormal activation of PI3K/AKT pathway. Multiple studies have demonstrated a key role of the PI3K/AKT signaling axis in the development of PCa and maintenance of CRPC [36, 37]. Until recently, however, results from clinical trials with AKT inhibitors in PCa have been largely disappointing. Crabb et al. showed that pan-AKT inhibitor capivasertib with docetaxel and prednisolone failed to improve progression-free survival in patients with mCRPC irrespective of PI3K/AKT/PTEN pathway activation status [8]. Therefore, an appropriate design of rational combinations of PI3K/AKT inhibitors with other novel agents is urgently needed.

Of note, many studies have shown that PTEN can synergize with other oncogenic factors or related genes in mouse models, including NKX3.1 [38], p27 [39], and p53 [40] to promote PCa development and androgen independence. Previously, we have demonstrated association of PTEN deletion with ERG rearrangement during PCa progression [5]. To the best of our knowledge, these observations suggested that a continuum rather than a stepwise mode of PTEN activity best described the process triggering tumor initiation and progression. In the current study, we discovered a novel reciprocal negative feedback regulation of ATF6α and PTEN that promotes PCa progression (Fig. 7). We demonstrated that 1) ATF6α is a novel negative regulator of PTEN by promoting PTEN protein degradation. 2) PTEN can shift the UPR pathway by selective inactivation of ATF6α. 3) Co-targeting ATF6α and AKT suppresses tumor cell proliferation and xenograft growth in PCa. These results highlighted co-targeting the AKT pathway and ATF6α oncogenic signaling as potential future therapies for PCa cases with PTEN

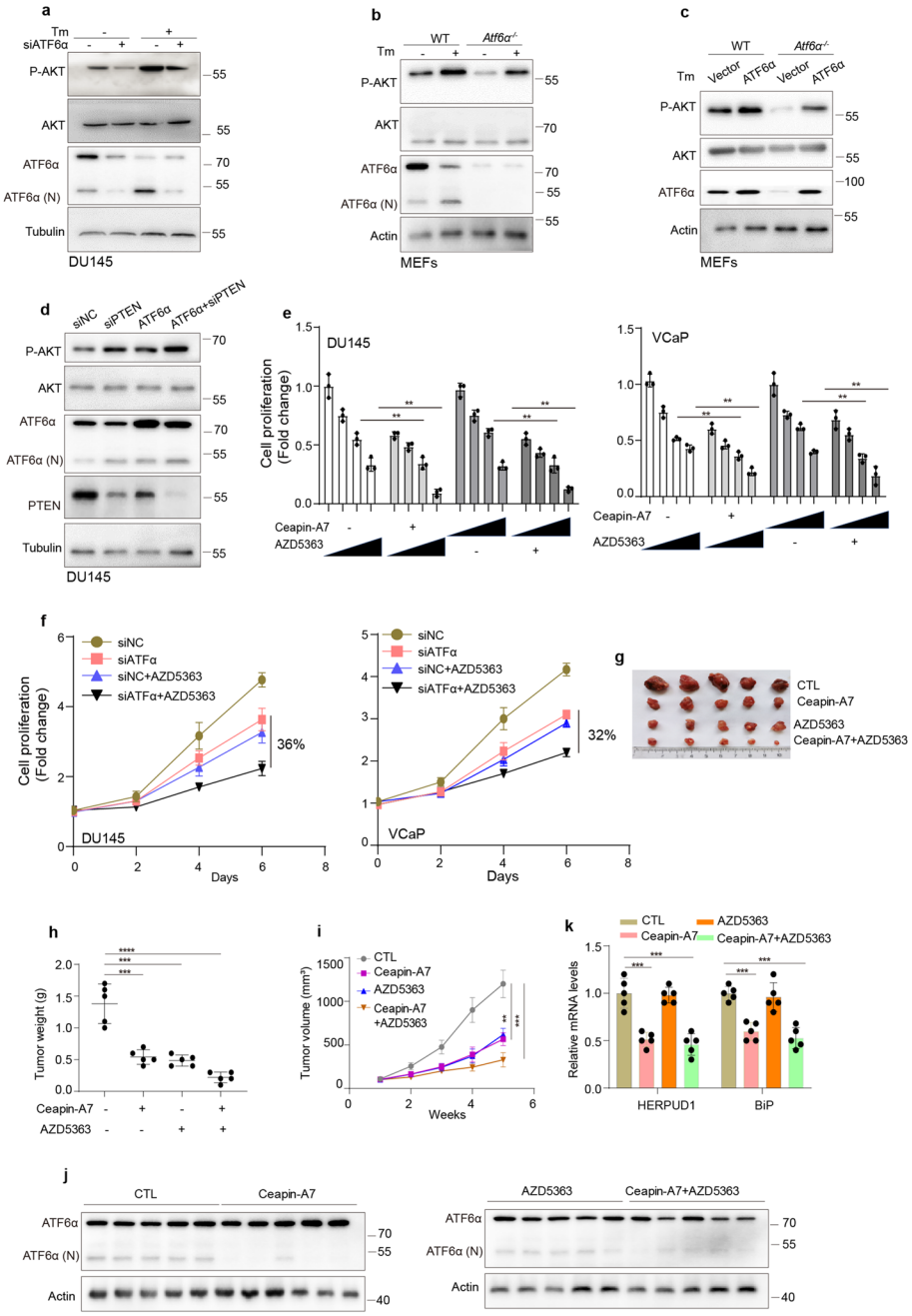

Fig. 6 Combined inhibition of ATF6α and AKT synergistically delays PCa progression with PTEN deficiency. **a** DU145 cells were transfected with siRNA against ATF6α for 48 h and then treated with 2.5 μM Tm for 12 h. The P-AKT and AKT protein levels were analyzed by western blot. **b** WT and *Atf6α*$^{-/-}$ MEFs were treated with Tm for 12 h. The P-AKT and AKT protein levels were analyzed by western blot. **c** WT and *Atf6α*$^{-/-}$ MEFs were transfected with ATF6α expression plasmid for 48 h and then treated with 2.5 μM Tm for 12 h. Whole cell lysates were then subjected to immunoblot analyses with indicated antibodies. **d** DU145 cells were transfected with siRNA against PTEN for 24 h and then transfected with ATF6α expression plasmid for another 48 h. Cells were lysed and blotted for P-AKT, AKT and tubulin. **e** DU145 cells were treated with increasing doses of AZD5363 (0, 5 μM, 10 μM, 20 μM) or Ceapin-A7 (0, 10 nM, 25 nM, 50 nM) alone or in combination with Ceapin-A7 (25 nM) or AZD5363 (10 μM), cell proliferation was detected by MTT at 72 h. **f** DU145 cells were transfected with siRNA against ATF6α for 24 h followed by AZD5363 treatment. Cell proliferation rates were measured by MTT. **g-i** Mice implanted with DU145 cells were treated with vehicle control, Ceapin-A7 (10 mg/kg), AZD5363 (100 mg/kg), or Ceapin-A7 + AZD5363 (n = 5). Tumor size was measured twice a week. At the endpoint, tumors isolated from euthanized mice were weighed and photographed. **j**, **k** The Xenograft tumors were collected 4 weeks after injection. The levels of endogenous ATF6α and its target genes in the excised tumors were determined by western blot and real time-qPCR analysis. Data represent mean ± SEM. P values were determined by two-tailed unpaired Student's t test; ** $P < 0.01$, *** $P < 0.001$, **** $P < 0.0001$

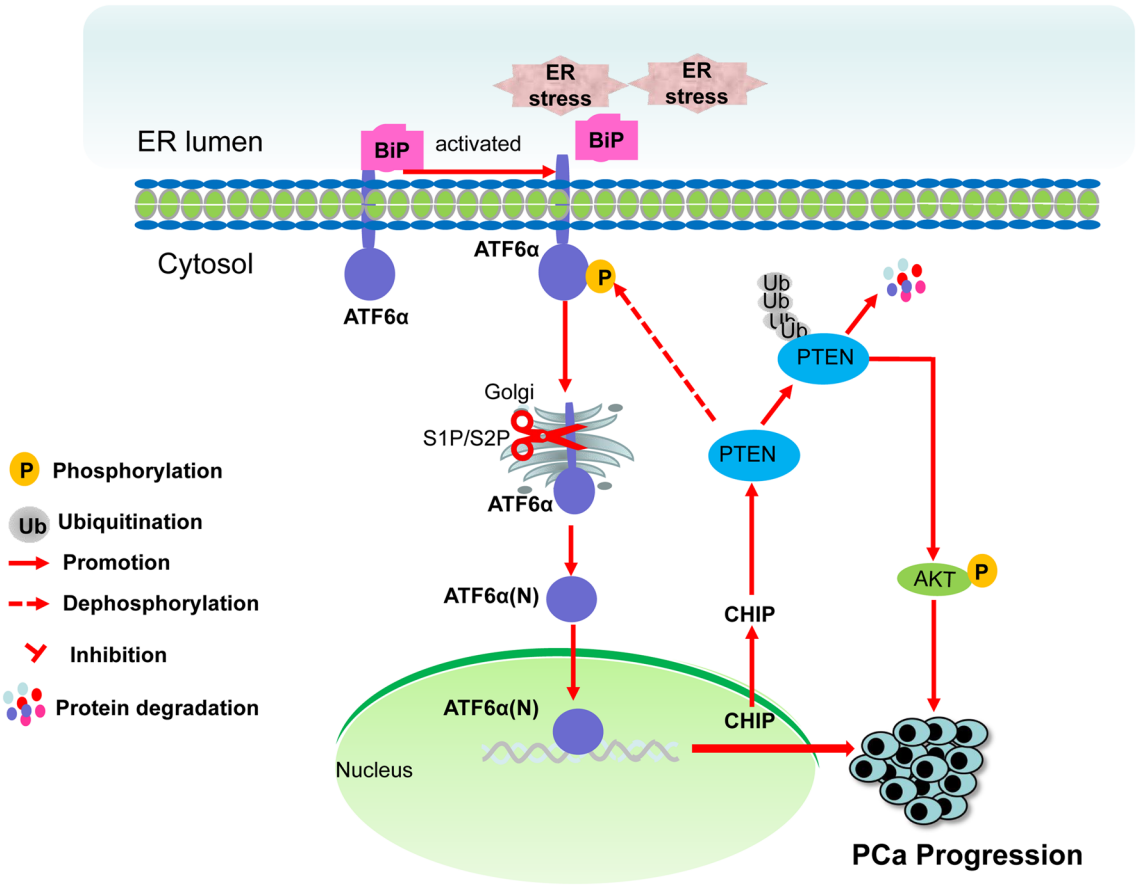

Fig. 7 Schematic representation of the ATF6α-PTEN axis in promote PCa progression. PTEN expression level was adversely correlated to ATF6α signaling in PCa. PTEN suppresses ATF6α activity by dephosphorylation, consequently inhibiting its nuclear translocation. In turn, ATF6α promotes PTEN ubiquitination degradation through CHIP

dysfunction. Indeed, while this study was in preparation, Yu et al. reported that PTEN phosphatase activity inhibits its metastasis by negatively regulating the Entpd5/IGF1R pathway through ATF6, thereby identifying novel candidate therapeutic targets for the treatment of PTEN mutant melanoma [41].

ATF6 is a transmembrane glycoprotein and transcription activator, which functions to initiate the UPR signaling during ER stress. The UPR is divided into three arms, including the PERK, ATF6 and IRE1. These three major effector proteins frequently cooperate in the transcriptional regulation of downstream targets. UPR signaling can affect various aspects of tumor cell biology, including angiogenesis, invasion, and therapy resistance [15]. Recent works have established that steroid hormone pathway, in particular androgens and estrogens related signaling, can regulate the UPR and enhance survival benefits for breast cancer and PCa cells [42]. In the current study, we demonstrated that UPR pathway is preferential activated in PTEN-deficient PCa. More importantly, ATF6α branch is closely related to PTEN dysfunction compared with that of PERK and IRE1. Functionally, silencing ATF6α, but not PERK or IRE1, can significantly attenuated the increase of cell proliferation induced by PTEN knockdown in vitro.

Although it has been documented that ATF6α is a major mammalian UPR sensor, there is limited data on the potential role of ATF6α in cancer progression. It was reported that activation of ATF6α can have both pro-survival and pro-death outcomes in cancers. There is evidence that ATF6α could drive cell proliferation in hepatoma cells [43], whereas knockdown of ATF6α in colon reduced cell proliferation [44]. However, in colorectal cancer cells, enforced expression of ATF6α reduced cell viability after exposure to low levels of Tg by reduced global protein synthesis [45]. ATF6 was also suggested to be involved in the process of UPR signaling-induced apoptotic pathways by the ER stress master regulator BiP/Grp78 [46]. Therefore, the exact role of ATF6α in tumors may be cell type- and context- specific. Our results showed overexpression of ATF6α increases the growth and colony formation of DU145 especially under the condition of Tm treatment. Wu et al. reported that exposure to either Tg or Tm significantly reduces the proliferative

capacity of ATF6α-/- cells relative to wild-type cells [47]. Most recently, Pachikov et al. reported that GCC185 played an important role in translocation of S1P and S2P proteases to the ER, which subsequent promoted ATF6 activity [48]. However, the exact role of ATF6α in PCa merit further investigation.

PTEN is a dual phosphatase with both protein and lipid phosphatase activities. PTEN has been reported to directly dephosphorylate residues on itself and others, to exert its tumour-suppressive function. PTEN deficiency is resulting mainly from PTEN deletion or mutation. However, PTEN can also be regulated at transcriptional, post-transcriptional and translation levels. Post-translational modifications, such as phosphorylation and ubiquitylation, have been shown to decrease PTEN protein levels [49]. Polyubiquitylation and monoubiquitylation play important roles in the regulation of PTEN degradation, in which NEDD4-1 [32], WWP2 [30], XIAP4 [31], and CHIP [29] are involved. Of them, CHIP is a highly conserved ubiquitin E3 ligase that can control the ubiquitination of multiple substrates, including p53, c-Myc, ErbB2, EGFR and PTEN [50]. In this study, our results demonstrated that PTEN inhibits the activity of ATF6α mainly by disturpting its phosphorylation at the Y111 site, while its lipid phosphatase is responsible for this function. Conversely, ATF6α promotes the ubiquitination and degradation of PTEN, thereby promoting cell proliferation.

Co-targeting strategies strive to improve cancer outcomes by combining therapies that selectively target exploitable alterations in tumor cells. In this study, we suggested that ATF6α and PTEN forms a negative feedback loop during PCa progression. It is, therefore, reasonable to believe that combinational therapies by co-targeting PI3K/AKT and other oncogenic pathways would provide optimal clinical benefits. We have shown evidence that co-treatment of ATF6α inhibitor (Ceapin-A7) and AKT inhibitor (AZD5363) resulted in stronger tumor suppression than AKT inhibitor alone. Our data demonstrated that co-targeting ATF6α and PI3K/AKT pathways may be a promising therapeutic approach for PCa, especially the ones with PTEN dysfunction.

Conclusions

In summary, ATF6α and PTEN forms a negative feedback loop during PCa progression. Combination of ATF6α inhibitor with AKT inhibitor suppresses tumor cell proliferation and xenograft growth. Importantly, this study highlighted ATF6α as a therapeutic vulnerability in PTEN dysfunctional PCa. Knowledge of the PTEN-ATF6α loop may prove to be valuable in the design of novel preventive and interventive therapeutic strategies in PCa.

Supplementary Information The online version contains supplementary material available at https://doi.org/10.1007/s00018-023-04940-3.

Author contributions BH, LW, TF, and RZ wrote the manuscript, performed, designed, and analyzed experiments; FS, HZ, and LG accomplished some of in vitro experiments; WC and MW analyzed experiments; TF, and YX accomplished some of in vivo studies; JH, MQ, JZ and LL analyzed IHC assay. All authors read and approved the final manuscript.

Funding This work was supported by the National Natural Science Foundation of China (Grants No. 82172818, 81972416), (Grant No. 81772760, 82072850), (Grant No. 81972436), Joint Research Fund of Natural Science of Shandong Province (ZR2019LZL014), Academic promotion program of Shandong First Medical University (LJ001), The Youth Innovation Technology Plan of Shandong University (Grant No. 2019KJK003), China Postdoctoral Science Foundation (2022M711900) and Natural Science Foundation of Shandong Province (ZR202111150013).

Data availability All data and material during the current study are available from the corresponding author on reasonable request.

Declarations

Conflict of interest The authors declare no competing interests.

Ethical approval This study was performed in line with the principles of the Declaration of Helsinki. Approval was granted by the Ethics Committee of Shandong University (Document No. ECSBMSSDU2021-1-61). All animal experimental protocols were performed following the Ethical Animal Care and Use Committee of Shandong University (Document No. ECSBMSSDU2021-2-126).

Consent to participate Informed consent was obtained from all individual participants included in the study.

Consent to publish The authors affirm that human research participants provided informed consent for publication of the images in Fig. 2a.

References

1. Barbieri CE et al (2013) The mutational landscape of prostate cancer. Eur Urol 64(4):567–576. https://doi.org/10.1016/j.eururo.2013.05.029
2. Li J et al (1997) PTEN, a putative protein tyrosine phosphatase gene mutated in human brain, breast, and prostate cancer. Science 275(5308):1943–1947. https://doi.org/10.1126/science.275.5308.1943
3. Alimonti A et al (2010) Subtle variations in Pten dose determine cancer susceptibility. Nat Genet 42(5):454–458. https://doi.org/10.1038/ng.556
4. Lotan TL et al (2011) PTEN protein loss by immunostaining: analytic validation and prognostic indicator for a high risk surgical cohort of prostate cancer patients. Clin Cancer Res 17(20):6563–6573. https://doi.org/10.1158/1078-0432.Ccr-11-1244
5. Han B et al (2009) Fluorescence in situ hybridization study shows association of PTEN deletion with ERG rearrangement during prostate cancer progression. Mod Pathol 22(8):1083–1093. https://doi.org/10.1038/modpathol.2009.69
6. Gray IC et al (1995) Loss of the chromosomal region 10q23-25 in prostate cancer. Cancer Res 55(21):4800–4803

7. Fruman DA, Rommel C (2014) PI3K and cancer: lessons, challenges and opportunities. Nat Rev Drug Discov 13(2):140–156. https://doi.org/10.1038/nrd4204
8. Crabb SJ et al (2021) Pan-AKT inhibitor Capivasertib With docetaxel and prednisolone in metastatic castration-resistant prostate cancer: a randomized, placebo-controlled phase II trial (ProCAID). J Clin Oncol 39(3):190–201. https://doi.org/10.1200/jco.20.01576
9. Cen B et al (2013) Elevation of receptor tyrosine kinases by small molecule AKT inhibitors in prostate cancer is mediated by Pim-1. Cancer Res 73(11):3402–3411. https://doi.org/10.1158/0008-5472.Can-12-4619
10. Chee KG et al (2007) The AKT inhibitor perifosine in biochemically recurrent prostate cancer: a phase II California/Pittsburgh cancer consortium trial. Clin Genitourin Cancer 5(7):433–437. https://doi.org/10.3816/CGC.2007.n.031
11. Sweeney C et al (2021) Ipatasertib plus abiraterone and prednisolone in metastatic castration-resistant prostate cancer (IPATential150): a multicentre, randomised, double-blind, phase 3 trial. Lancet 398(10295):131–142. https://doi.org/10.1016/s0140-6736(21)00580-8
12. Yuan L et al (2015) Deubiquitylase OTUD3 regulates PTEN stability and suppresses tumorigenesis. Nat Cell Biol 17(9):1169–1181. https://doi.org/10.1038/ncb3218
13. Bassi C et al (2013) Nuclear PTEN controls DNA repair and sensitivity to genotoxic stress. Science 341(6144):395–399. https://doi.org/10.1126/science.1236188
14. Goel A et al (2004) Frequent inactivation of PTEN by promoter hypermethylation in microsatellite instability-high sporadic colorectal cancers. Cancer Res 64(9):3014–3021. https://doi.org/10.1158/0008-5472.can-2401-2
15. Hetz C et al (2020) Mechanisms, regulation and functions of the unfolded protein response. Nat Rev Mol Cell Biol 21(8):421–438. https://doi.org/10.1038/s41580-020-0250-z
16. Sheng X et al (2019) IRE1α-XBP1s pathway promotes prostate cancer by activating c-MYC signaling. Nat Commun 10(1):323. https://doi.org/10.1038/s41467-018-08152-3
17. de la Calle CM et al (2022) The endoplasmic reticulum stress response in prostate cancer. Nat Rev Urol 19(12):708–726. https://doi.org/10.1038/s41585-022-00649-3
18. Chui MH et al (2019) Chromosomal instability and mTORC1 activation through PTEN loss contribute to Proteotoxic stress in Ovarian carcinoma. Cancer Res 79(21):5536–5549. https://doi.org/10.1158/0008-5472.Can-18-3029
19. Wang W et al (2018) KDM4B-regulated unfolded protein response as a therapeutic vulnerability in PTEN-deficient breast cancer. J Exp Med 215(11):2833–2849. https://doi.org/10.1084/jem.20180439
20. Haze K et al (2001) Identification of the G13 (cAMP-response-element-binding protein-related protein) gene product related to activating transcription factor 6 as a transcriptional activator of the mammalian unfolded protein response. Biochem J 355(Pt 1):19–28. https://doi.org/10.1042/0264-6021:3550019
21. Forouhan M et al (2018) Paradoxical roles of ATF6α and ATF6β in modulating disease severity caused by mutations in collagen X. Matrix Biol. https://doi.org/10.1016/j.matbio.2018.03.004
22. Liu J et al (2017) Activation of UPR signaling pathway is associated with the malignant progression and poor prognosis in prostate cancer. Prostate 77(3):274–281. https://doi.org/10.1002/pros.23264
23. Wang L et al (2013) SOX4 is associated with poor prognosis in prostate cancer and promotes epithelial-mesenchymal transition in vitro. Prostate Cancer Prostatic Dis 16(4):301–307. https://doi.org/10.1038/pcan.2013.25
24. Feng T et al (2016) Growth factor progranulin promotes tumorigenesis of cervical cancer via PI3K/Akt/mTOR signaling pathway. Oncotarget. https://doi.org/10.18632/oncotarget.11126
25. Plate L et al (2016) Small molecule proteostasis regulators that reprogram the ER to reduce extracellular protein aggregation. eLife https://doi.org/10.7554/eLife.15550.
26. Myers MP et al (1998) The lipid phosphatase activity of PTEN is critical for its tumor supressor function. Proc Natl Acad Sci U S A 95(23):13513–13518. https://doi.org/10.1073/pnas.95.23.13513
27. Maehama T, Dixon JE (1998) The tumor suppressor, PTEN/MMAC1, dephosphorylates the lipid second messenger, phosphatidylinositol 3,4,5-trisphosphate. J Biol Chem 273(22):13375–13378. https://doi.org/10.1074/jbc.273.22.13375
28. Lee YR et al (2018) The functions and regulation of the PTEN tumour suppressor: new modes and prospects. Nat Rev Mol Cell Biol 19(9):547–562. https://doi.org/10.1038/s41580-018-0015-0
29. Ahmed SF et al (2012) The chaperone-assisted E3 ligase C terminus of Hsc70-interacting protein (CHIP) targets PTEN for proteasomal degradation. J Biol Chem 287(19):15996–16006. https://doi.org/10.1074/jbc.M111.321083
30. Maddika S et al (2011) WWP2 is an E3 ubiquitin ligase for PTEN. Nat Cell Biol 13(6):728–733. https://doi.org/10.1038/ncb2240
31. Van Themsche C et al (2009) X-linked inhibitor of apoptosis protein (XIAP) regulates PTEN ubiquitination, content, and compartmentalization. J Biol Chem 284(31):20462–20466. https://doi.org/10.1074/jbc.C109.009522
32. Wang X et al (2007) NEDD4-1 is a proto-oncogenic ubiquitin ligase for PTEN. Cell 128(1):129–139. https://doi.org/10.1016/j.cell.2006.11.039
33. Misra J et al (2013) Transcriptional cross talk between orphan nuclear receptor ERRγ and transmembrane transcription factor ATF6α coordinates endoplasmic reticulum stress response. Nucleic Acids Res 41(14):6960–6974. https://doi.org/10.1093/nar/gkt429
34. Zhang W et al (2015) Feedback regulation on PTEN/AKT pathway by the ER stress kinase PERK mediated by interaction with the Vault complex. Cell Signal 27(3):436–442. https://doi.org/10.1016/j.cellsig.2014.12.010
35. Rebello RJ et al (2021) Prostate cancer. Nat Rev Dis Primers 7(1):9. https://doi.org/10.1038/s41572-020-00243-0
36. Ferraldeschi R et al (2015) PTEN protein loss and clinical outcome from castration-resistant prostate cancer treated with abiraterone acetate. Eur Urol 67(4):795–802. https://doi.org/10.1016/j.eururo.2014.10.027
37. Toren P et al (2015) Combination AZD5363 with Enzalutamide significantly delays Enzalutamide-resistant prostate cancer in preclinical models. Eur Urol 67(6):986–990. https://doi.org/10.1016/j.eururo.2014.08.006
38. Kim MJ et al (2002) Cooperativity of Nkx3.1 and Pten loss of function in a mouse model of prostate carcinogenesis. Proc Natl Acad Sci USA 99(5):2884–2889. https://doi.org/10.1073/pnas.042688999
39. Di Cristofano A et al (2001) Pten and p27KIP1 cooperate in prostate cancer tumor suppression in the mouse. Nat Genet 27(2):222–224. https://doi.org/10.1038/84879
40. Chen Z et al (2005) Crucial role of p53-dependent cellular senescence in suppression of Pten-deficient tumorigenesis. Nature 436(7051):725–730. https://doi.org/10.1038/nature03918
41. Yu Y, et al (2023) PTEN phosphatase inhibits metastasis by negatively regulating the Entpd5/IGF1R pathway through ATF6. iScience 26 (2): 106070 https://doi.org/10.1016/j.isci.2023.106070.
42. Jin Y, Saatcioglu F (2020) Targeting the unfolded protein response in hormone-regulated cancers. Trends Cancer 6(2):160–171. https://doi.org/10.1016/j.trecan.2019.12.001
43. Vandewynckel YP et al (2016) Next-generation proteasome inhibitor oprozomib synergizes with modulators of the unfolded

protein response to suppress hepatocellular carcinoma. Oncotarget 7(23):34988–35000. https://doi.org/10.18632/oncotarget.9222
44. Benedetti R et al (2022) ATF6 prevents DNA damage and cell death in colon cancer cells undergoing ER stress. Cell Death Discov 8(1):295. https://doi.org/10.1038/s41420-022-01085-3
45. Spaan CN et al (2019) Expression of UPR effector proteins ATF6 and XBP1 reduce colorectal cancer cell proliferation and stemness by activating PERK signaling. Cell Death Dis 10(7):490. https://doi.org/10.1038/s41419-019-1729-4
46. Verfaillie T et al (2013) Targeting ER stress induced apoptosis and inflammation in cancer. Cancer Lett 332(2):249–264. https://doi.org/10.1016/j.canlet.2010.07.016
47. Wu J et al (2007) ATF6alpha optimizes long-term endoplasmic reticulum function to protect cells from chronic stress. Dev Cell 13(3):351–364. https://doi.org/10.1016/j.devcel.2007.07.005
48. Pachikov AN et al (2021) The non-canonical mechanism of ER stress-mediated progression of prostate cancer. J Exp Clin Cancer Res 40(1):289. https://doi.org/10.1186/s13046-021-02066-7
49. Salmena L et al (2008) Tenets of PTEN tumor suppression. Cell 133(3):403–414. https://doi.org/10.1016/j.cell.2008.04.013
50. Wu HH et al (2021) Hsp70 acts as a fine-switch that controls E3 ligase CHIP-mediated TAp63 and ΔNp63 ubiquitination and degradation. Nucleic Acids Res 49(5):2740–2758. https://doi.org/10.1093/nar/gkab081